HHS Public Access

Author manuscript

Environ Sci Technol. Author manuscript; available in PMC 2022 November 03.

Published in final edited form as:

Environ Sci Technol. 2022 February 01; 56(3): 1743–1752. doi:10.1021/acs.est.1c06796.

Utility of Diffusive Gradient in Thin-Film (DGT) Passive Samplers for Predicting Mercury Methylation Potential and Bioaccumulation in Freshwater Wetlands

Natalia Neal-Walthall[1], **Udonna Ndu**[1,2], **Nelson A. Rivera Jr.**[1], **Dwayne A. Elias**[3], **Heileen Hsu-Kim**[1,*]

[1]Department of Civil and Environmental Engineering, Duke University, Box 90287, Durham, North Carolina 27708, United States

[2]Harte Research Institute for Gulf of Mexico Studies, Texas A&M Corpus Christi, Corpus Christi, TX, 78412, United States

[3]Elias Consulting, LLC, Knoxville, Tennessee 37934, United States

Abstract

Mercury is a risk in aquatic ecosystems when the metal is converted to methylmercury (MeHg) and subsequently bioaccumulates in aquatic food webs. This risk can be difficult to manage because of the complexity of biogeochemical processes for mercury and the need for accessible techniques to navigate this complexity. Here, we explored the use of diffusive gradient in thin-film (DGT) passive samplers as a tool to simultaneously quantify the methylation potential of inorganic Hg (IHg) and the bioaccumulation potential of MeHg in freshwater wetlands. Outdoor freshwater wetland mesocosms were amended with four isotopically labelled and geochemically relevant IHg forms that represent a range of methylation potentials ($^{202}Hg^{2+}$, ^{201}Hg-humic acid, ^{199}Hg-sorbed to FeS, ^{200}HgS nanoparticles). Six weeks after the spikes, we deployed DGT samplers in the mesocosm water and sediments, evaluated DGT-uptake rates of total Hg, MeHg, and IHg (calculated by difference) for the Hg isotope spikes, and examined correlations with total Hg, MeHg, and IHg concentrations in sediment, water, and micro- and macrofauna in the ecosystem. In the sediments, we observed greater relative MeHg concentrations from the initially dissolved IHg isotope spikes and lower MeHg levels from the initially particulate IHg spikes. These trends were consistent with uptake flux of IHg into DGTs deployed in surface sediments. Moreover, we observed correlations between total Hg-DGT uptake flux and MeHg levels in periphyton biofilms, submergent plant stems, snails and mosquitofish in the ecosystem. These correlations were better for DGTs deployed in the water column compared to DGTs in the sediments, suggesting the importance of vertical distribution of bioavailable MeHg in relation to food sources for macrofauna. Overall, these results demonstrate that DGT passive samplers are

*Corresponding Author: hsukim@duke.edu, +1(919) 660-5109.

Supporting Information:

Additional details of Methods including the preparation of Hg isotope stock solutions, establishment of the wetland mesocosm, sample collection, and chemical analysis methods. Additional Results include general water quality characteristics of the wetlands, statistical analyses of endmember distributions in sediment and DGT samplers, and mercury concentration values predicted by the DGTs compared to measured soluble concentrations.

The authors declare no competing financial interest.

a relatively simple and efficient tool for predicting IHg methylation and MeHg bioaccumulation potentials without the need to explicitly delineate IHg and MeHg speciation and partitioning in complex ecosystems.

Graphical Abstract

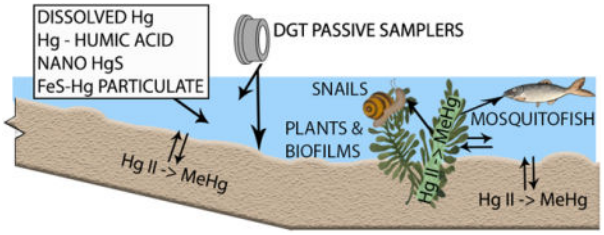

Keywords

methylmercury; bioavailability; passive sampling; sediments; periphyton; biofilm

INTRODUCTION

Mercury (Hg) is an aquatic contaminant of broad concern, particularly in ecosystems where inorganic forms of Hg are converted to monomethylmercury (MeHg), a bioaccumulative and neurotoxic form of the metal.[1, 2] MeHg biomagnifies in the aquatic food web, resulting in MeHg levels in fish and other aquatic food sources that pose dietary exposure risks for humans and wildlife.[3] The chemical speciation of inorganic divalent Hg (IHg) is important to environmental processes that drive the production of MeHg in the environment. For example, methylation of IHg is largely mediated by anaerobic microorganisms that frequently inhabit low oxygen environments such as aquatic sediments, saturated soils, and anoxic microzones found within biofilms.[4–6] In these habitats, the dominant forms of IHg typically include Hg(II) complexed with dissolved and particulate natural organic matter (NOM) and Hg(II) associated with mineral phases (i.e., sulfides).[7] The bioavailability of IHg for methylation depends on the chemical lability of IHg species in these habitats.[8–10]

The distribution and speciation of MeHg are also key factors for the bioaccumulation of MeHg in the aquatic food web. MeHg concentrations in aquatic organisms can be highly variable between different locations.[11–14] While such differences are partly attributed to localized ecosystem food web structure and dietary preferences, the bioavailability of MeHg at key entry points of the food web is also an important driver.[3, 15] MeHg species are comprised of sorbed and aqueous complexes of CH_3Hg^+, which generally entail coordination to thiolate moieties associated with NOM.[16, 17]

With the multiple interconnected processes that influence the speciation and distribution of IHg and MeHg in aquatic ecosystems, better methods are needed to simplify the prediction of IHg bioavailability for methylation and MeHg bioaccumulation potential in aquatic food webs. Here, we studied diffusive gradient in thin film (DGT) passive samplers as a potential tool for time-integrated sampling of IHg and MeHg bioavailability in freshwater ecosystems. A DGT sampler for mercury consists of a plastic device that encase three layers: an outer

filter (0.45 μm nominal pore size) exposed to the sampling medium, a middle diffusion gel layer, and the innermost metal-binding layer comprising a thiolated resin.[18] Mercury uptake rates in DGTs are presumed to correspond to average soluble IHg and MeHg concentrations during the sampling period; however, researchers have debated how to convert measured mass uptake data to soluble concentrations.[19–26] Instead, we posit that DGT data may be more useful if they can directly relate to IHg biomethylation and MeHg biouptake potentials, linkages that have been studied but yet to be firmly established.

For example in our recent work, we showed that methylation of IHg spiked into sediment slurries correlated with IHg accumulation rate on DGTs.[27] We hypothesized that the agarose gel layer provides a size exclusion mechanism that might mimic transport of IHg across an extracellular polymer network at the cell envelope of methylating microorganisms, limiting the uptake to soluble, chemically labile IHg forms. While several studies have evaluated DGTs for predicting IHg methylation potential[27] and bioaccumulation of Hg species (either MeHg or IHg)[26, 28–32], most of these studies involved laboratory observations (e.g., jar and aquarium incubations). The utility of DGTs for evaluating IHg methylation potential has yet to be firmly demonstrated in complex aquatic ecosystems where diel/seasonal cycles and hydrological conditions influence mercury biogeochemical transformations.[24] We also note that while three of the studies evaluating DGTs for predicting Hg bioaccumulation in aquatic organisms were conducted in natural environments[26, 28, 32], all were conducted in riverine ecosystems. To our knowledge, DGT prediction of Hg bioaccumulation in wetland ecosystems has yet to be examined despite the fact that wetlands are often hotspots for MeHg production and a source of MeHg to aquatic food webs.[33, 34]

The objective of this study was to evaluate the efficacy of DGT passive samplers for monitoring IHg methylation potential and MeHg bioaccumulation potential in experimental freshwater wetlands. In this work, we sought to test two overarching hypotheses: (1) IHg accumulation rate into DGTs deployed in surface sediments and surface water are predictive of IHg methylation potential in wetland sediment and periphyton; and (2) MeHg accumulation rate in DGTs deployed in sediment and/or surface water of the wetland correlate with MeHg concentrations in macro- and microfauna (aquatic plants, snails, fish, and periphyton biofilms). To test these hypotheses, we constructed 3 outdoor freshwater wetland mesocosms that were amended with multiple isotopically labelled, geochemically relevant IHg species: two soluble forms ($^{202}Hg^{2+}$ and ^{201}Hg(II)-humic acid) and two particulate forms (nanocrystalline ^{200}HgS aggregates and ^{199}Hg(II) adsorbed to FeS particles). These forms are expected to span a range of mobility and methylation potential.[27, 35, 36] Six weeks after IHg additions, we monitored each isotopically labelled Hg endmember for: (1) total Hg (TotHg) and MeHg concentrations in sediment and water; (2) bioaccumulation of MeHg in periphyton biofilms, snails, stem/leaves of submergent aquatic plants, and adult mosquitofish in the mesocosm ecosystem; and (3) accumulation rate of TotHg and MeHg on DGTs deployed for a one week period in sediment and water. IHg concentrations and uptake rate into DGTs were determined by difference of TotHg and MeHg. The data were then used to evaluate the ability of mercury-DGT uptakes rate to predict MeHg production and bioaccumulation.

MATERIALS AND METHODS

Freshwater Wetland Mesocosms - Design and Construction

The wetland mesocosms were located at the outdoor Duke Forest experimental facility (Durham, North Carolina, USA). These mesocosms are based on the same design described in previous research evaluating contaminant bioaccumulation[37–39] and are described in detail in the Supporting Information (SI). In brief, for this study we utilized six wetland mesocosms, each comprising a slant bottom box (3.7 × 1.2 × 0.8 m^3), lined with a polymer fabric, and filled with a 25 cm layer of sandy loam soil (Sands and Soil, Durham, NC) and water from a local groundwater well. A variety of emergent and submergent macrophytes were planted in the soil. Notably, the permanently saturated aquatic zone (with water levels ranging from 20–30 cm during the experiment) was populated with the submergent water weed *Egeria densa*. The wetland was also colonized by associated microbial communities, insects, locally prevalent freshwater snails (*Physella sp. and Lymnaea sp.*), and eastern mosquitofish (*Gambusia holbrookii*). The mesocosms boxes were located in a fenced clearing of the forest and were open to the atmosphere for the duration of this study. After maturation, three randomly assigned mesocosms were dosed with Hg (Box 1–3) and three were used as undosed controls (C1–3).

Addition of Isotopically Labelled Hg(II) Species to Wetland Mesocosms

Stock solutions of the isotopically labelled Hg forms (or 'endmembers') were the following: (1) Dissolved $^{202}Hg^{2+}$ in 5% nitric acid; (2) ^{201}Hg(II)-humic acid mixture formulated with 103 nmol ^{201}Hg per 1 mg organic C as Suwannee River NOM (International Humic Substances Society Product# 2R101N); (3) Nanoparticulate ^{200}HgS (26 nm average hydrodynamic diameter); and (4) ^{199}Hg(II) adsorbed to FeS (Figure S1), synthesized with 179 μmol ^{199}Hg per gram of freshly formed FeS particles. The Supporting Information describes the isotopic composition of each enriched Hg isotope stock as well as their synthesis and characterization.

In early August 2017 (3 months after mesocosm construction), surface sediment and water from each mesocosm were collected for analysis of baseline TotHg contents. Then on August 15, 2017, aliquots of each Hg stock solution (corresponding to 12 mg Hg of each isotopically labelled 'endmember') were added to the overlying water of the aquatic zone in the mesocosm box. This mass of Hg was selected for a target concentration of ~100 ng Hg g^{-1} per isotope endmember in the top 4 cm of sediment (assuming complete deposition to this layer for each spike) across the submerged portion of the mesocosm. The rationale for dosing is based on the following: 1) similar TotHg sediment levels have been observed in urban ecosystems or near legacy industrial contamination[40]; 2) previous experiments at this mesocosm facility demonstrated that spikes of nanoparticle suspensions primarily accumulated in the surface sediments after several weeks[38, 39, 41]; and 3) the need to exceed measured ambient TotHg levels for isotope tracing. The average ± standard deviation pre-dosing levels were 16.7 ± 3.2 ng g^{-1} for sediments and 11.4 ± 9.8 ng L^{-1} for surface water. Details for dosing procedure may be found in the SI.

Note that while each Hg isotope spike initially comprised a well-defined Hg form (i.e., dissolved or particulate), upon addition to the mesocosm the speciation and distribution of Hg from each spike was expected to change via biogeochemical transformations (e.g., sorption, settling, complexation, precipitation/dissolution, oxidation/reduction). The extent of these transformations was expected to be different for each spike.[27, 35, 36]

Sample Collection and Processing

Circular piston-style DGTs were constructed (described in the SI) and deployed face down in the surface sediment (n=6) and suspended in the water column (n=12) in each mesocosm box at five weeks after the Hg dosing. The samplers were deployed for one week to maximize exposure time without imparting great risk of biofouling, which has previously been observed for deployment times of 10 days and greater.[42] After samplers were retrieved, surface water (n=6), sediment (n=3), and biota including mosquitofish (n=4), snails (n=6), submerged *E. densa* aquatic plant stems (n=4) and associated periphyton biofilms were collected. Surface water was collected in acid cleaned glass vessels, stored on ice for transport to the lab, then filtered with 0.2 μm poly(ether sulfone) filter (VWR), and frozen for later chemical analyses (TotHg, MeHg, dissolved organic carbon, and major anion concentrations).

In the lab, fish and snails were rinsed with deionized water. *E. densa* stems were submerged and shaken with deionized water to remove biofilm material, and this material was concentrated to a moist pellet by centrifugation. The remaining plant material was then rinsed with deionized water and massaged with gloved hands to ensure thorough removal of all residual biofilms. Plants, biofilm pellets, fish and snails were freeze-dried and stored frozen until analysis for MeHg content. The DGT samplers that were deployed in sediments were disassembled in the laboratory, and the resin layers were cut in two halves, weighed, and stored separately for TotHg and MeHg analysis. For the DGT samplers deployed in surface water, the resin layer from each sampler was saved as an intact sample for either TotHg or MeHg analysis (resulting in n=6 samples for each analysis).

Sediment was collected from predetermined locations (Figure S2) as intact cores in acid clean plastic tubes. The top 2 cm was removed, homogenized, and frozen as separate aliquots for later analysis of TotHg, MeHg content, wet/dry ratio, and loss on ignition (LOI) as described in SI. In addition, the surface water depth, temperature, specific conductance, pH, and dissolved O_2 content were assessed *in situ* at multiple times over the 6-week period after Hg dosing.

Chemical Analyses

Details for all chemical analyses are available in the SI section. In brief, the resin layer of the DGT samplers and sediment samples were processed for TotHg analysis by room temperature aqua regia digestion for a minimum of 24 hour. Surface water samples for TotHg analysis were preserved with 0.5% BrCl. The samples were then analyzed for isotope specific TotHg content by stannous chloride reduction, amalgamation (BrooksRand T-MERX) coupled with inductively coupled plasma mass spectrometry (ICP-MS, Agilent Technologies 7700 series).

For MeHg analyses, biological samples were extracted with 4 M nitric acid heated to 55 °C for 16 hours.[43] Water samples were processed by distillation.[44] DGT resin layer and sediment samples were processed by acidified potassium bromide /dichloromethane extraction.[45] Extracts were analyzed for isotope-specific MeHg by ethylation, purge-and-trap gas chromatography (BrooksRand M-MERX) followed by ICP-MS. TotHg and MeHg contents from each isotopically-labelled Hg spike was calculated by matrix deconvolution based on the known isotopic compositions of the four Hg spikes and the measured isotopic composition in the sample.[46] TotHg and MeHg contents in biological and sediment samples are reported in units of ng (as Hg) per dry sample mass.

The DGT data are reported as a mass flux (ng Hg cm^{-2} d^{-1}) by taking the TotHg and MeHg mass measured on the DGT resin layer and normalizing to the exposed DGT sampler surface (3.14 cm^2), the weight of the resin layer sample fragment relative to the total resin layer weight (for sediment-deployed DGTs), and deployment time (7 days). IHg content was determined by difference between TotHg and MeHg contents in the sample. Metal uptake flux into DGT samplers is influenced by the soluble metal concentration and diffusion rate as well as resupply of soluble metal in the water through desorption/dissolution reactions during the DGT deployment period.[18, 47, 48 20, 49] Thus, we interpret this flux value to represent the amount of chemically-labile Hg (originating from both aqueous and particulate forms) at the DGT sampling surface.

Major anions (Cl^-, SO_4^{2-}, Br^-, NO_3^-) concentrations in filtered surface water samples were quantified by ion chromatography (Dionex ICS-2000). Dissolved organic carbon was analyzed by combustion catalytic oxidation/non-dispersive infrared spectroscopy (Shimadzu TOC-V).

Data Analyses

Sediment IHg and MeHg contents from each isotope endmember were compared by calculating, for each sediment replicate sample, the fraction of each endmember contributing to the total IHg and MeHg (based on the sum of all four endmembers). The fraction from each endmember was also calculated for DGT-IHg and DGT-MeHg flux for samplers deployed in sediments. The fractions were compared by analysis of variance (ANOVA) with a post-hoc Tukey's Honestly Significant Difference Test to determine if the fractions contributed by the isotope endmembers were significantly difference from each other (defined at α=0.05).

Relationships between continuous variables (i.e., DGT flux, mercury concentrations in sediment and biological samples) were assessed by linear least squares regression. For data groups that did not meet normal distribution requirements for regression, $\log_{10}$ transformations of the data were applied prior to regression analyses. Regressions were performed to compare sediment MeHg content from each isotope spiked to both sediment IHg content and DGT-IHg uptake flux. In addition, linear regressions were performed to compare MeHg concentrations in biota (biofilms, *E. densa*, snails, and fish) to DGT-TotHg and DGT-MeHg uptake fluxes in water and DGT-MeHg in sediment. Data analysis and figure production were performed in R (Version 1.2.5001).[50]

RESULTS AND DISCUSSION

IHg and MeHg Concentration and DGT-Uptake Flux in Sediment

Upon addition of the 4 isotopically labelled IHg species to the wetland mesocosms (labelled as Box 1, 2 and 3 in Figure 1), a large portion of the added mercury from each endmember was observed in the surface sediment layer six weeks after the spike addition. The average sediment IHg content (calculated by different between measured TotHg and MeHg values) for each isotope endmember in each mesocosm box ranged from 50 to 594 ng/g (Figure 1a). We observed substantial variability of sediment IHg contents (and TotHg) in triplicate samples collected from the same mesocosm box, as shown by the error bars representing 1 standard error of the average.

We estimated the percentage of the added Hg spikes that partitioned to sediments assuming the following: 1) the added mercury was distributed across the submerged aquatic zone (1.68 m^2) with a penetration depth of 4 cm (based on previous studies of nanomaterial addition to similar wetland mesocosms[38]; and 2) the *in situ* bulk density was 1.6 g cm^{-3} for loosely consolidated sediment (based on previous observations[51]). With these assumptions and the measured sediment concentrations of TotHg, we estimated that 46% to 550% of the initial Hg spikes were present in this compartment. This result suggests substantial accumulation of the Hg spikes in the aquatic zone sediments, which is consistent with previous work involving other metal species spiked into similarly designed wetland mesocosms.[38, 39] In this study as in previous work, the Hg isotope spikes were heterogeneously distributed in sediments. Thus, we recognize that more precise estimates for the fraction of added Hg in the surface sediments were not possible.

Despite the variability of IHg contents across the aquatic zone sediments, the relative abundance of IHg originating from each isotope spike at 6 weeks post-dosing was generally the same in each mesocosm, regardless of overall IHg concentration, as shown in Figure 1a, Figure S3, and supported by an analysis of variance of the data (SI Section 6). Although the IHg isotope spikes were added to the mesocosms as separate solutions, they were each injected at the same points immediately below the surface water. Thus, the sediment IHg results suggest that the method of IHg application did not result in substantial concentration variation between the isotope spikes at a single sediment location. However, the method of Hg introduction resulted in substantial horizontal variation for the total added Hg (i.e., the sum of all 4 Hg endmembers). The amount of spatial heterogeneity in the sediments is consistent with similar mesocosm experiments at this facility involving the addition of nanomaterials.[38]

In contrast to the isotope endmember distribution of sediment IHg, MeHg concentrations in sediment were greater for the mercury originating from the dissolved endmembers ($^{202}Hg^{2+}$, ^{201}Hg-humic acid complex) than the initially particulate endmembers (nanoparticulate ^{200}HgS and ^{199}Hg adsorbed to FeS) (Figure 1b and Figure S3). This trend was also observed in accumulation rates of both IHg and MeHg into DGTs deployed in the sediments: DGT flux of IHg and MeHg was greater for dissolved endmembers than particulate endmembers (Figures 1c, 1d, and S4). These trends between DGT uptake flux of IHg and methylation

potential are similar to results observed in previous laboratory experiments performed with sediment slurries.[27, 36]

Note that the average sediment IHg concentration was greater in Box 1 than in the other mesocosms boxes while the DGT-flux of IHg was relatively similar between boxes. We attribute this disparity to the large heterogeneity of the surface sediments and the relatively small number of replicate samples (n=3) collected for TotHg sediment analysis compared to more replicate DGT samplers (n=6) deployed in the sediment zone.

TotHg and MeHg Concentrations and DGT-Uptake Flux in Surface Water

Concentrations of both TotHg and MeHg in filtered surface water were greater for the mercury originating from the dissolved endmembers ($^{202}Hg^{2+}$, ^{201}Hg-humic acid complex) than the initially particulate endmembers (nanoparticulate ^{200}HgS and ^{199}Hg adsorbed to FeS) (Figure 2a and 2b). MeHg was approximately 5% of TotHg, indicating that most of the TotHg was IHg in filtered surface water. With the relatively low amount of MeHg in the surface water, here we report TotHg-DGT flux rather than the calculated IHg-DGT flux for the surface water DGTs, with the understanding that most of this is IHg and also that field applications of DGTs more frequently quantify TotHg and not IHg. The results showed that the relative contribution from each isotope endmember to the surface water TotHg (Figure 2a) is consistent with the trends observed in DGT flux of TotHg for the four isotope endmembers (Figure 2c). This trend is different than observed in sediments, where DGT-uptake flux of IHg was greater for the dissolved than the particulate endmembers even though sediment IHg concentrations was roughly equal for all endmembers (Figures 1, S3 and S4).

These observations highlight that TotHg concentration in surface water is a more reliable measure of the mobile or chemically labile form of the metal than concentrations in sediment. However, we note that MeHg concentrations in water obtained from Box 2 were significantly higher (almost double) than measured concentrations in Boxes 1 and 3. This trend was not observed in sediment MeHg concentrations, but was observed in periphyton biofilms (described in the next section), suggesting that biofilms rather than sediments were the source of MeHg in surface water. Such difference between boxes were not observed in MeHg accumulated in water-deployed DGTs.

In addition to TotHg and MeHg concentrations in surface water, we observed other general water quality characteristics that were similar to previous experiments at this facility (Table S2 and S3). Water temperature measured weekly at the 9 to 11 am period was between 17–26 °C, and water depth (between 23.5 – 29 cm) was consistent between replicate mesocosm boxes. Measured dissolved organic carbon (DOC) was between 5.3–33.5 mg/L while the pH during this time of day was 8.5 to 9.3. Sulfate, which can enhance MeHg levels in freshwater ecosystems,[52] was slightly lower in concentration in Box 2 (2.9–4 mg/L) compared to Boxes 1 and 3 (3.6–5.4 mg/L). This observation does not explain the greater level of surface water MeHg in Box 2 compared to the other boxes.

With this understanding of general water quality characteristics, we calculated concentration values for soluble MeHg and TotHg from the DGT flux data by using a previously

described[18] solute diffusive uptake equation (SI Section 7). The results were consistent for measured TotHg in filtered surface water but tended to underpredict measured MeHg concentrations (average predicted values were 59% ± 15% of measured) (Figure S5). These inconsistencies highlight the challenges of using DGT flux data for predicting soluble concentrations of mercury. The calculations involved diffusion coefficients measured for surrogate IHg- and MeHg-humic species that are presumed to represent soluble IHg and MeHg species in our system. These predictions also require assumptions that solute transport into the DGTs occur under constant temperature, which may not be relevant given diel fluctuations that could influence temperatures in the relatively shallow wetland mesocosms. Our prior work also showed that colloidal sulfide particles can deposit on the filter or gel layer of the DGT and decrease uptake rate of soluble Hg(II) on the DGT resin layer.[53] We could not rule out a similar process occurring with suspended colloids (such as colloidal organic matter) in the mesocosms. Because of these uncertainties, we did not utilize the calculated soluble TotHg and MeHg concentrations for further analysis. Instead, we used the DGT uptake flux values for subsequent comparisons to mercury levels in biological specimens.

Distribution of MeHg in Wetland Fauna

MeHg contents in all biota (periphyton biofilms, *E. densa* stems/leaves, snails, and adult mosquitofish) were greater for mercury originating from initially dissolved isotope endmembers compared to the initial particulate endmembers (Figure 3). In addition, bioaccumulation followed expected trends in that measured concentrations of MeHg in higher trophic level organisms (fish and snails) were greater than MeHg concentrations in lower trophic level organisms (periphyton biofilms and aquatic plants).

Although we managed and sampled the replicate mesocosm boxes with the same methods, we observed differences between boxes, indicating variability between replicate ecosystems. While this study was a Hg-spike experiment in a constructed wetland ecosystem, MeHg levels in the biological specimens are comparable to those observed in studies of natural systems. MeHg concentrations in periphyton (~75 to 250 ng/g) were similar to or higher than previously observed values (1 to 300 ng/g dw) for periphyton obtained from a variety of freshwater ecosystems (e.g., streams, rivers, lakes, wetlands).[26, 54–57] TotHg and MeHg concentrations in surface water samples of our mesocosms were higher than observed in all but one of these prior studies. Regardless, MeHg concentrations in snails and mosquitofish in our mesocosms are similar to other experimental dosing studies and in freshwater ecosystems near an industrial point source of mercury[26, 58, 59]. However, Hg concentrations in mosquitofish are higher in our study than in wetland ecosystems without a known mercury point source.[54]

Correlations between MeHg/IHg Levels and Uptake Flux in DGTs

In the sediments, MeHg contents for each endmember did not correlate with sediment IHg content ($p = 0.23$) (Figure 4). Instead, IHg flux into DGTs was moderately predictive of sediment MeHg contents ($p = 0.021$, $r^2 = 0.43$). We observed similar trends previously in laboratory sediment slurries[27], although the correlations were stronger in the lab study compared to this study. Key differences with the prior work are the shorter period (7 days)

and the experimental design that enabled relatively homogenous replicate slurries. In the present study, we evaluated three distinct wetland ecosystems, each with heterogeneous distribution of Hg in the sediment. Despite the complexities of the wetland ecosystem structure, our results showed that IHg-DGT flux correlated with sediment MeHg content, indicating that the DGT samplers were probing the IHg forms that were bioavailable to methylating microorganisms in sediments.

Because sediments were an important source of MeHg in the wetland mesocosms, we hypothesized that MeHg concentrations in macrofauna would depend on the labile fraction of MeHg in surface sediment (as indicated by MeHg flux into DGTs). The sediment DGT data was positively correlated with MeHg in fish ($p=0.013$) and aquatic plants ($p=0.031$). However, we observed poor correlations between sediment DGT data and MeHg in snails ($p=0.63$) and periphyton biofilms ($p=0.27$) (Figure 5 A–D). A relationship was not expected in the case of biofilms given the potential for *in situ* MeHg production in the biofilms.[6, 60–63]

While the MeHg-DGT flux in sediments showed mixed results for correlations with MeHg levels in the biological specimens, the surface water DGT data showed improved correlations. MeHg-DGT flux correlated strongly with MeHg contents in periphyton biofilms, aquatic plants, snails, and fish ($p < 0.05$ for all) (Figure 5 E–H). Other studies in estuaries and streams have shown similar results in that MeHg concentrations in fish and other pelagic species correlated with MeHg levels in surface water rather than MeHg in sediments, which are typically the MeHg hotspots.[43, 64, 65] Our results demonstrate that even for a relatively shallow wetland environment, the vertical distribution of MeHg is important for controlling bioavailability for micro- and macrofauna in the ecosystem.

Finally, DGT uptake flux of TotHg from surface water was generally the best predictor for MeHg levels in biota ($p \leq 0.01$ for all) (Figure 5 I–L). The strong correlation with periphyton biofilms could indicate that TotHg-DGT uptake flux is a measure of both labile MeHg available for direct accumulation and labile IHg available for *in situ* methylation in the biofilm. The strong correlations observed between TotHg uptake in water deployed DGTs and MeHg concentration in plants, snails, and fish were not expected. These results could reflect the pathways in which MeHg accumulate in these macrofauna and highlight the importance of periphyton biofilms for this process. For example, MeHg in the biofilms could partition into the *E. densa* tissue via leaf pores, as shown to occur with gold ion complexes in prior studies.[37, 66] Likewise, the periphyton biofilms in the mesocosms could be the major source of food for snails and mosquitofish in the ecosystem. This has been previously observed for both organisms.[26, 54, 55] Thus, the DGT parameter to best correlate with MeHg in the biofilms (i.e., the surface water TotHg-DGT flux) also produced the strongest correlations with MeHg in other macrofauna.

Environmental Relevance

The results of this study support the use of DGT passive samplers for monitoring IHg methylation potential and MeHg bioaccumulation potential in freshwater wetlands. When IHg is introduced into an ecosystem, a myriad of biogeochemical transformations and transport processes control the accumulation of MeHg in sediment and wetland fauna. The extent of these processes is particularly relevant for ecosystems that receive multiple

IHg inputs of varying speciation, mobility, and chemical lability (e.g., soluble, weakly complexed IHg species from recent atmospheric deposition; chemically inert IHg associated with sulfides in mobilized soil particles). Despite the complexity of these processes, we observed that IHg-DGT flux could be used to predict methylation potential of multiple IHg sources to a wetland, and TotHg-DGT flux could be predictive of MeHg bioaccumulation potential in wetland organisms without the need to explicitly delineate IHg and MeHg speciation and partitioning in complex ecosystems. We also showed that the vertical placement of the DGTs (i.e., sediment versus surface water) influenced the quality of the correlations, suggesting that the location of sampling should consider whether MeHg bioaccumulation is primarily of benthic or pelagic origin.

Several previous studies have attempted to correlate TotHg or MeHg DGT data with MeHg levels in biological specimens. Many of these studies, however, involved benthic organisms and sediment deployed DGTs.[29, 67, 68] Moreover, previous studies generally involved lab experiments or ecosystems where differences between surface water and sediment for sampler deployment were not examined.[26, 29–31, 67, 68] Here, our study enabled a direct comparison of locations for DGT deployment and demonstrated the importance of sampling in surface water instead of sediment. A recent study in a stream ecosystem by Xu *et al.*[26] reported correlations between surface water DGTs and periphyton, similar to our study here. A key difference, however, is that we observed much greater periphyton MeHg levels relative to surface water TotHg/MeHg concentrations in our wetland mesocosms than observed in the Xu *et al.* study. Such differences likely stem from contrasting hydrological and biogeochemical conditions in lotic and lentic aquatic ecosystems that influence solute transport, physical structure, and community composition within biofilms. The application of DGT data for prediction of mercury bioaccumulation potential will need to consider such conditions.

While this study demonstrates the efficacy of DGT samplers for monitoring mercury in aquatic ecosystems, DGT data alone provide an incomplete picture. The methylation potential of IHg depends not only on the bioavailability of IHg (as the DGTs might help quantify), but also on the composition and activity of microbial methylators. This study examined MeHg levels at a single time point, but over longer time scales and seasonal cycles the abundance and activity of microbial methylators is likely to change in the wetlands. In addition, the decomposition of MeHg needs to be considered.

For the accumulation of MeHg in the periphyton biofilms and other wetland fauna, the DGT data might be useful in the development of bioaccumulation models. For example, if the MeHg-DGT flux data are converted to soluble MeHg concentrations, the parameter could be useful for calculation of bioaccumulation factors or MeHg trophic transfer. This approach would require assumptions regarding diffusive uptake of soluble MeHg species in the DGT samplers, potentially introducing unnecessary error as noted above. An alternative approach could directly link mercury-DGT flux with bioaccumulation rate in a biodynamic model that is calibrated to local food web dynamics and feeding patterns. Altogether, our work highlights promising applications of DGT samplers for indicating IHg methylation and MeHg bioaccumulation potentials. An ecosystem model for mercury bioaccumulation

potential could help the long-standing challenge of evaluating the key factors controlling MeHg levels in the aquatic environment.

Supplementary Material

Refer to Web version on PubMed Central for supplementary material.

Acknowledgements

This study was supported by the National Institute of Environmental Health Sciences Superfund Research Program (R01ES24344, P42ES010356), the Center for Environmental Implications of NanoTechnology supported by the National Science Foundation and the Environmental Protection Agency (DBI-1266252), and the U.S. Department of Energy, Office of Science Biological and Environmental Research program (DE-SC0019408). We thank Dr. Nick Geitner for his assistance in mesocosm construction and Ms. Brooke Hassett and the Duke River Center for their assistance with anion and DOC analyses.

References

1. Rudd JWM; Kelly CA; Beaty KG; Flett RJ; St. Louis VL; Bloom NS, Importance of Wetlands as Sources of Methyl Mercury to Boreal Forest Ecosystems. Canadian Journal of Fisheries and Aquatic Sciences 1994, 51, (5), 1065–1076.
2. Hurley JP; Benoit JM; Babiarz CL; Shafer MM; Andren AW; Sullivan JR; Hammond R; Webb DA, Influences of watershed characteristics on mercury levels in wisconsin rivers. Environmental science & technology 1995, 29, (7), 1867–1875. [PubMed: 22176462]
3. Eagles-Smith CA; Silbergeld EK; Basu N; Bustamante P; Diaz-Barriga F; Hopkins WA; Kidd KA; Nyland JF, Modulators of Mercury Risk to Wildlife and Humans in the Context of Rapid Global Change. Ambio 2018, 47, (2), 170–197. [PubMed: 29388128]
4. Dranguet P; Slaveykova VI; Faucheur SL, Kinetics of mercury accumulation by freshwater biofilms. Environmental chemistry (Online) 2017, 14, (7), 458.
5. Dranguet P; Le Faucheur S; Cosio C; Slaveykova VI, Influence of chemical speciation and biofilm composition on mercury accumulation by freshwater biofilms. Environmental science. Processes & impacts 2017, 19, (1), 38–49. [PubMed: 27942649]
6. Olsen TA; Brandt CC; Brooks SC, Periphyton Biofilms Influence Net Methylmercury Production in an Industrially Contaminated System. Environmental Science & Technology 2016, 50, (20), 10843–10850. [PubMed: 27617484]
7. Hsu-Kim H; Kucharzyk KH; Zhang T; Deshusses MA; Subsurface Biogeochemical, R., Mechanisms regulating mercury bioavailability for methylating microorganisms in the aquatic environment: a critical review. Environmental science & technology 2013, 47, (6), 2441–2456. [PubMed: 23384298]
8. Thomas SA; Mishra B; Myneni SCB, Cellular Mercury Coordination Environment, and Not Cell Surface Ligands, Influence Bacterial Methylmercury Production. Environmental Science & Technology 2020, 54, (7), 3960–3968. [PubMed: 32097551]
9. Adediran GA; Liem-Nguyen V; Song Y; Schaefer JK; Skyllberg U; Björn E; Sveriges l., Microbial Biosynthesis of Thiol Compounds: Implications for Speciation, Cellular Uptake, and Methylation of Hg(II). Environmental Science & Technology 2019, 53, (14), 8187–8196. [PubMed: 31257868]
10. Wang Y; Janssen SE; Schaefer JK; Yee N; Reinfelder JR, Tracing the Uptake of Hg(II) in an Iron-Reducing Bacterium Using Mercury Stable Isotopes. Environmental Science & Technology Letters 2020, 7, (8), 573–578.
11. Chen C; Amirbahman A; Fisher N; Harding G; Lamborg C; Nacci D; Taylor D, Methylmercury in Marine Ecosystems: Spatial Patterns and Processes of Production, Bioaccumulation, and Biomagnification. EcoHealth 2008, 5, (4), 399–408. [PubMed: 19015919]
12. Yoshino K; Mori K; Kanaya G; Kojima S; Henmi Y; Matsuyama A; Yamamoto M, Food Sources are More Important Than Biomagnification on Mercury Bioaccumulation in Marine Fishes. Environmental Pollution (1987) 2020, 262, 113982–113982.

13. Gentès S; Löhrer B; Legeay A; Mazel AF; Anschutz P; Charbonnier C; Tessier E; Maury-Brachet R, Drivers of Variability in Mercury and Methylmercury Bioaccumulation and Biomagnification in Temperate Freshwater Lakes. Chemosphere (Oxford) 2021, 267, 128890–128890.

14. Evers DC; Sauer AK; Burns DA; Fisher NS; Bertok DC; Adams EM; Burton MEH, A Synthesis of Patterns of Environmental Mercury Inputs, Exposure and Effects in New York State. Ecotoxicology (London) 2020, 29, (10), 1565–1589.

15. Gorski PR; Armstrong DE; Hurley JP; Shafer MM, Speciation of Aqueous Methylmercury Influences Uptake by a Freshwater Alga (Selenastrum capricornutum). Environmental Toxicology and Chemistry 2006, 25, (2), 534–540. [PubMed: 16519317]

16. Hintelmann H; Welbourn PM; Evans RD, Measurement of Complexation of Methylmercury(II) Compounds by Freshwater Humic Substances Using Equilibrium Dialysis. Environmental Science & Technology 1997, 31, (2), 489–495.

17. Liem-Nguyen V; Skyllberg U; Björn E; Sveriges l., Thermodynamic Modeling of the Solubility and Chemical Speciation of Mercury and Methylmercury Driven by Organic Thiols and Micromolar Sulfide Concentrations in Boreal Wetland Soils. Environmental Science & Technology 2017, 51, (7), 3678–3686. [PubMed: 28248107]

18. Zhang D. a., Progress in understanding the use of diffusive gradients in thin films (DGT) – back to basics. Environ. Chem 2012, (9), 1–13.

19. Diviš P; Leermakers M; Dočekalová H; Gao Y, Mercury Depth Profiles in River and Marine Sediments Measured by the Diffusive Gradients in Thin Films Technique with Two Different Specific Resins. Analytical and Bioanalytical Chemistry 2005, 382, (7), 1715–1719. [PubMed: 16021421]

20. Clarisse O; Dimock B; Hintelmann H; Best EPH, Predicting net mercury methylation in sediments using diffusive gradient in thin films measurements. Environmental science & technology 2011, 45, (4), 1506–1512. [PubMed: 21222459]

21. Fernández-Gómez C; Dimock B; Hintelmann H; Díez S, Development of the DGT Technique for Hg Measurement in Water: Comparison of Three Different Types of Samplers in Laboratory Assays. Chemosphere 2011, 85, (9), 1452–1457. [PubMed: 21925697]

22. Noh S; Kim Y.-h.; Kim H; Seok K.-s.; Park M; Bailon MX; Hong Y, The Performance of Diffusive Gradient in Thin Film Probes for the Long-Term Monitoring of Trace Level Total Mercury in Water. Environmental Monitoring and Assessment 2020, 192, (1), 1.

23. Bratkič A; Klun K; Gao Y, Mercury Speciation in Various Aquatic Systems Using Passive Sampling Technique of Diffusive Gradients in Thin-Film. Science of the Total Environment 2019, 663, 297–306. [PubMed: 30711596]

24. Bretier M; Dabrin A; Billon G; Mathon B; Miège C; Coquery M, To What Extent Can the Biogeochemical Cycling of Mercury Modulate the Measurement of Dissolved Mercury in Surface Freshwaters by Passive Sampling? Chemosphere (Oxford) 2020, 248, 126006–126006.

25. Díez S; Giaggio R, Do biofilms affect the measurement of mercury by the DGT technique? Microcosm and field tests to prevent biofilm growth. Chemosphere (Oxford) 2018, 210, 692–698.

26. Xu X; Bryan AL; Mills GL; Korotasz AM, Mercury Speciation, Bioavailability, and Biomagnification in Contaminated Streams on the Savannah River Site (SC, USA). The Science of the Total Environment 2019, 668, 261. [PubMed: 30852203]

27. Ndu U; Christensen GA; Rivera NA; Gionfriddo CM; Deshusses MA; Elias DA; Hsu-Kim H, Quantification of Mercury Bioavailability for Methylation Using Diffusive Gradient in Thin-Film Samplers. Environmental science & technology 2018, 52, (15), 8521–8529. [PubMed: 29920204]

28. Pisanello F; Marziali L; Rosignoli F; Poma G; Roscioli C; Pozzoni F; Guzzella L, In Situ Bioavailability of DDT and Hg in Sediments of the Toce River (Lake Maggiore basin, Northern Italy): Accumulation in Benthic Invertebrates and Passive Samplers. Environmental Science and Pollution Research International 2016, 23, (11), 10542–10555. [PubMed: 26662101]

29. Amirbahman A; Massey DI; Lotufo G; Steenhaut N; Brown LE; Biedenbach JM; Magar VS, Assessment of Mercury Bioavailability to Benthic Macroinvertebrates Using Diffusive Gradients in Thin Films (DGT). Environmental Science. Processes & Impacts 2013, 15, (11), 2104. [PubMed: 24084872]

30. Pelcová P; Vičarová P; Dočekalová H; Poštulková E; Kopp R; Mareš J; Smolíková V, The Prediction of Mercury Bioavailability for Common Carp (Cyprinus carpio L.) using the DGT Technique in the Presence of Chloride Ions and Humic Acid. Chemosphere 2018, 211, 1109–1112. [PubMed: 30223326]

31. Clarisse O; Lotufo GR; Hintelmann H; Best EPH, Biomonitoring and Assessment of Monomethylmercury Exposure in Aqueous Systems using the DGT Technique. Science of the Total Environment 2012, 416, 449–454. [PubMed: 22221872]

32. Marziali L; Valsecchi L, Mercury Bioavailability in Fluvial Sediments Estimated Using Chironomus riparius and Diffusive Gradients in Thin-Films (DGT). Environments 2021, 8, (2), 7.

33. Hall BD; Aiken GR; Krabbenhoft DP; Marvin-DiPasquale M; Swarzenski CM, Wetlands as Principal Zones of Methylmercury Production in Southern Louisiana and the Gulf of Mexico Region. Environmental Pollution (1987) 2008, 154, (1), 124–134.

34. St. Louis VL; Rudd JWM; Kelly CA; Beaty KG; Bloom NS; Flett RJ, Importance of Wetlands as Sources of Methyl Mercury to Boreal Forest Ecosystems. Canadian Journal of Fisheries and Aquatic Sciences 1994, 51, (5), 1065–1076.

35. Jonsson S; Skyllberg U; Nilsson MB; Westlund P-O; Shchukarev A; Lundberg E; Björn E, Mercury Methylation Rates for Geochemically Relevant HgII Species in Sediments. Environmental Science & Technology 2012, 46, (21), 11653–11659. [PubMed: 23017152]

36. Jonsson S; Skyllberg U; Nilsson MB; Lundberg E; Andersson A; Björn E, Differentiated Availability of Geochemical Mercury Pools Controls Methylmercury Levels in Estuarine Sediment and Biota. Nature Communications 2014, 5, (1), 4624–4624.

37. Avellan A; Simonin M; McGivney E; Bossa N; Spielman-Sun E; Rocca JD; Bernhardt ES; Geitner NK; Unrine JM; Wiesner MR; Lowry GV, Gold Nanoparticle Biodissolution by a Freshwater Macrophyte and its Associated Microbiome. Nature Nanotechnology 2018, 13, (11), 1072–1077.

38. Geitner NK; Cooper JL; Avellan A; Castellon BT; Perrotta BG; Bossa N; Simonin M; Anderson SM; Inoue S; Hochella MF; Richardson CJ; Bernhardt ES; Lowry GV; Ferguson PL; Matson CW; King RS; Unrine JM; Wiesner MR; Hsu-Kim H, Size-Based Differential Transport, Uptake, and Mass Distribution of Ceria (CeO2) Nanoparticles in Wetland Mesocosms. Environmental Science & Technology 2018, 52, (17), 9768–9776. [PubMed: 30067347]

39. Avellan A; Simonin M; Anderson SM; Geitner NK; Bossa N; Spielman-Sun E; Bernhardt ES; Castellon BT; Colman BP; Cooper JL; Ho M; Hochella MF; Hsu-Kim H; Inoue S; King RS; Laughton S; Matson CW; Perrotta BG; Richardson CJ; Unrine JM; Wiesner MR; Lowry GV, Differential Reactivity of Copper- and Gold-Based Nanomaterials Controls Their Seasonal Biogeochemical Cycling and Fate in a Freshwater Wetland Mesocosm. Environmental Science & Technology 2020, 54, (3), 1533–1544. [PubMed: 31951397]

40. Hsu-Kim H; Eckley CS; Achá D; Feng X; Gilmour CC; Jonsson S; Mitchell CPJ; Duke Univ, D. N. C.; Institutionen för miljövetenskap och analytisk, k.; Stockholms, u.; Naturvetenskapliga, f., Challenges and opportunities for managing aquatic mercury pollution in altered landscapes. Ambio 2018, 47, (2), 141–169. [PubMed: 29388127]

41. Colman BP; Baker LF; King RS; Matson CW; Unrine JM; Marinakos SM; Gorka DE; Bernhardt ES, Dosing, Not the Dose: Comparing Chronic and Pulsed Silver Nanoparticle Exposures. Environmental Science & Technology 2018, 52, (17), 10048–10056. [PubMed: 30075078]

42. Díez S; Giaggio R, Do biofilms affect the measurement of mercury by the DGT technique? Microcosm and field tests to prevent biofilm growth. Chemosphere 2018, 210, 692–698. [PubMed: 30031999]

43. Chen CY; Borsuk ME; Bugge DM; Hollweg T; Balcom PH; Ward DM; Williams J; Mason RP, Benthic and pelagic pathways of methylmercury bioaccumulation in estuarine food webs of the northeast United States. PloS one 2014, 9, (2), e89305. [PubMed: 24558491]

44. Method 1630: Methylmercury in Water by Distillation, Aqueous Ethylation, Purge and Trap, and CVAFS. In US Environmental Protection Agency, Ed. Washington, DC, 1998.

45. Qian J; Skyllberg U; Tu Q; Bleam WF; Frech W, Efficiency of Solvent Extraction Methods for the Determination of Methylmercury in Forest Soils. Fresenius' Journal of Analytical Chemistry 2000, 367, (5), 467–473. [PubMed: 11227478]

46. Hintelmann H; Evans RD, Application of Stable Isotopes in Environmental Tracer Studies – Measurement of Monomethylmercury (CH3Hg+) by Isotope Dilution ICP-MS and Detection of Species Transformation. Fresenius' Journal of Analytical Chemistry 1997, 358, (3), 378–385.
47. Zhang H; Davison W, Performance Characteristics of Diffusion Gradients in Thin Films for the in Situ Measurement of Trace Metals in Aqueous Solution. Analytical Chemistry (Washington) 1995, 67, (19), 3391–3400.
48. Clarisse O; Hintelmann H, Measurements of Dissolved Methylmercury in Natural Waters using Diffusive Gradients in Thin Film (DGT). Journal of Environmental Monitoring 2006, 8, (12), 1242. [PubMed: 17133281]
49. Xie M; Simpson SL; Huang J; Teasdale PR; Wang W-X, In Situ DGT Sensing of Bioavailable Metal Fluxes to Improve Toxicity Predictions for Sediments. Environmental Science & Technology 2021, 55, (11), 7355–7364. [PubMed: 33973770]
50. Ihaka R; Gentleman R, R: A Language for Data Analysis and Graphics. Journal of Computational and Graphical Statistics 1996, 5, (3), 299–314.
51. Hsu RT; Liu JT, In-situ estimations of the density and porosity of flocs of varying sizes in a submarine canyon. Marine geology 2010, 276, (1–4), 105–109.
52. Gilmour CC; Henry EA; Mitchell R, Sulfate Stimulation of Mercury Methylation in Freshwater Sediments. Environmental Science & Technology 1992, 26, (11), 2281–2287.
53. Pham AL-T; Johnson C; Manley D; Hsu-Kim H; Duke Univ, D. N. C., Influence of Sulfide Nanoparticles on Dissolved Mercury and Zinc Quantification by Diffusive Gradient in Thin-Film Passive Samplers. Environmental Science & Technology 2015, 49, (21), 12897–12903. [PubMed: 26414810]
54. Liu G; Cai Y; Philippi T; Kalla P; Scheidt D; Richards J; Scinto L; Appleby C, Distribution of Total and Methylmercury in Different Ecosystem Compartments in the Everglades; implications for Mercury Bioaccumulation. Environmental Pollution (1987) 2008, 153, (2), 257–265.
55. Xiang Y; Liu G; Yin Y; Cai Y, Periphyton as an Important Source of Methylmercury in Everglades Water and Food Web. Journal of Hazardous Materials 2021, 410, 124551–124551. [PubMed: 33223320]
56. Roxanna Razavi N; Cushman SF; Halfman JD; Massey T; Beutner R; Cleckner LB, Mercury bioaccumulation in stream food webs of the Finger Lakes in central New York State, USA. Ecotoxicology and environmental safety 2019, 172, 265–272. [PubMed: 30711861]
57. Desrosiers M; Planas D; Mucci A, Total mercury and methylmercury accumulation in periphyton of Boreal Shield Lakes: Influence of watershed physiographic characteristics. The Science of the total environment 2006, 355, (1), 247–258. [PubMed: 15894350]
58. Walters DM; Raikow DF; Hammerschmidt CR; Mehling MG; Kovach A; Oris JT, Methylmercury Bioaccumulation in Stream Food Webs Declines with Increasing Primary Production. Environmental Science & Technology 2015, 49, (13), 7762–7769. [PubMed: 26018982]
59. Pickhardt PC; Stepanova M; Fisher NS, Contrasting Uptake Routes and Tissue Distributions of Inorganic and Methylmercury in Mosquitofish (Gambusia affinis) and Redear Sunfish (Lepomis microlophus). Environmental Toxicology and Chemistry 2006, 25, (8), 2132–2142. [PubMed: 16916033]
60. Hamelin S; Planas D; Amyot M, Mercury Methylation and Demethylation by Periphyton Biofilms and their Host in a Fluvial Wetland of the St. Lawrence River (QC, Canada). The Science of the Total Environment 2015, 512–513, 464–471.
61. Hamelin S. p.; Amyot M; Barkay T; Wang Y; Planas D, Methanogens: Principal Methylators of Mercury in Lake Periphyton. Environmental Science & Technology 2011, 45, (18), 7693–7700. [PubMed: 21875053]
62. Bouchet S; Goñi-Urriza M; Monperrus M; Guyoneaud R. m.; Fernandez P; Heredia C; Tessier E; Gassie C; Point D; Guédron S. p.; Achá D; Amouroux D, Linking Microbial Activities and Low-Molecular-Weight Thiols to Hg Methylation in Biofilms and Periphyton from High-Altitude Tropical Lakes in the Bolivian Altiplano. Environmental Science & Technology 2018, 52, (17), 9758–9767. [PubMed: 30037219]

63. Bae H-S; Dierberg FE; Ogram A, Periphyton and Flocculent Materials Are Important Ecological Compartments Supporting Abundant and Diverse Mercury Methylator Assemblages in the Florida Everglades. Applied and Environmental Microbiology 2019, 85, (13).

64. Taylor VF; Buckman KL; Seelen EA; Mazrui NM; Balcom PH; Mason RP; Chen CY, Organic carbon content drives methylmercury levels in the water column and in estuarine food webs across latitudes in the Northeast United States. Environmental Pollution 2019, 246, 639–649. [PubMed: 30605819]

65. Chasar LC; Scudder BC; Stewart AR; Bell AH; Aiken GR, Mercury cycling in stream ecosystems. 3. Trophic dynamics and methylmercury bioaccumulation. Environmental science & technology 2009, 43, (8), 2733–2739. [PubMed: 19475942]

66. Stegemeier JP; Avellan A; Lowry GV, Effect of Initial Speciation of Copper- and Silver-Based Nanoparticles on Their Long-Term Fate and Phytoavailability in Freshwater Wetland Mesocosms. Environmental Science & Technology 2017, 51, (21), 12114–12122. [PubMed: 29017014]

67. Pisanello F; Marziali L; Rosignoli F; Poma G; Roscioli C; Pozzoni F; Guzzella L, In situ bioavailability of DDT and Hg in sediments of the Toce River (Lake Maggiore basin, Northern Italy): Accumulation in Benthic invertebrates and Passive Samplers. Environmental Science and Pollution Research International 2015, 23, (11), 10542–10555. [PubMed: 26662101]

68. Marziali L; Valsecchi L, Mercury Bioavailability in Fluvial Sediments Estimated Using Chironomus riparius and Diffusive Gradients in Thin-Films (DGT). Environments (Basel, Switzerland) 2021, 8, (2), 7.

Non-technical Synopsis:

Diffusive gradient in thin-film passive samplers can effectively quantify bioaccumulative forms of mercury in aquatic ecosystem and assist the mitigation of environmental mercury pollution.

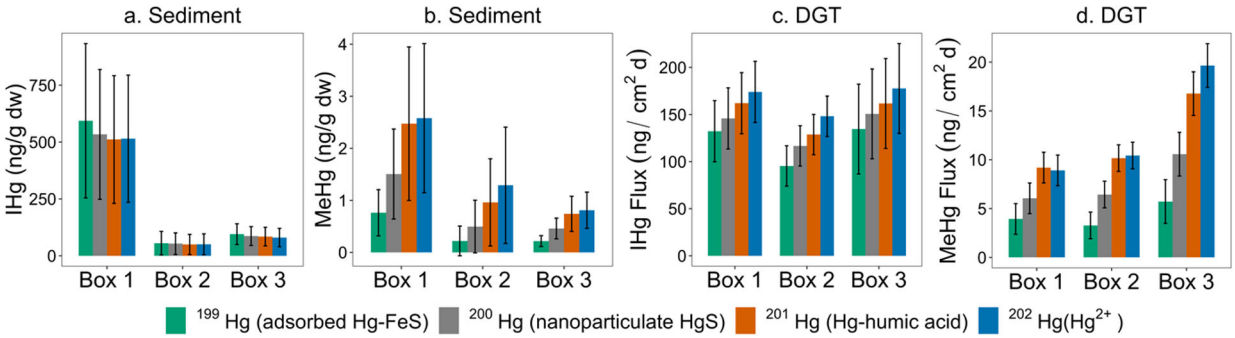

Figure 1.

(a) Sediment inorganic Hg (IHg) and (b) Sediment methylmercury (MeHg) contents from each Hg isotope spike added to triplicate wetland mesocosms (Box 1, Box 2, and Box 3) and quantified 6 weeks after the initial Hg isotope dosing. (c) and (d) Uptake rate into sediment deployed DGTs. Each bar represents the average ± standard error.

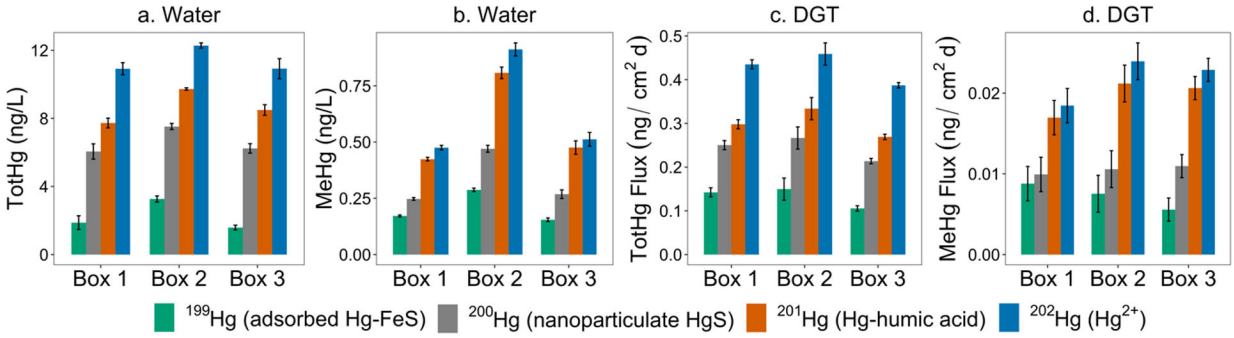

Figure 2.

Filtered surface water concentrations of (a) Total Hg in water (TotHg) and (b) Methylmercury in water (MeHg) from each Hg isotope spike added to each wetland mesocosm box and quantified at 6 weeks after the initial Hg isotope dosing. (c) and (d) Uptake rate into surface water deployed DGTs. Each bar represents the average ± standard error.

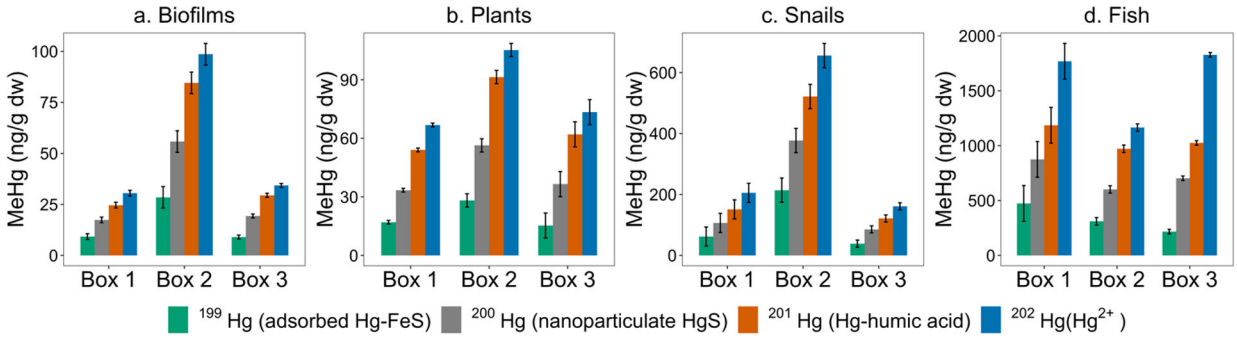

Figure 3.

MeHg content from each Hg isotope spike in fauna of the wetland mesocosms: (a) Periphyton biofilms; (b) *E. densa* plant stem and leaves; (c) Snails; (d) Mosquitofish (*Gambusia* sp.). Each bar represents the average ± standard error.

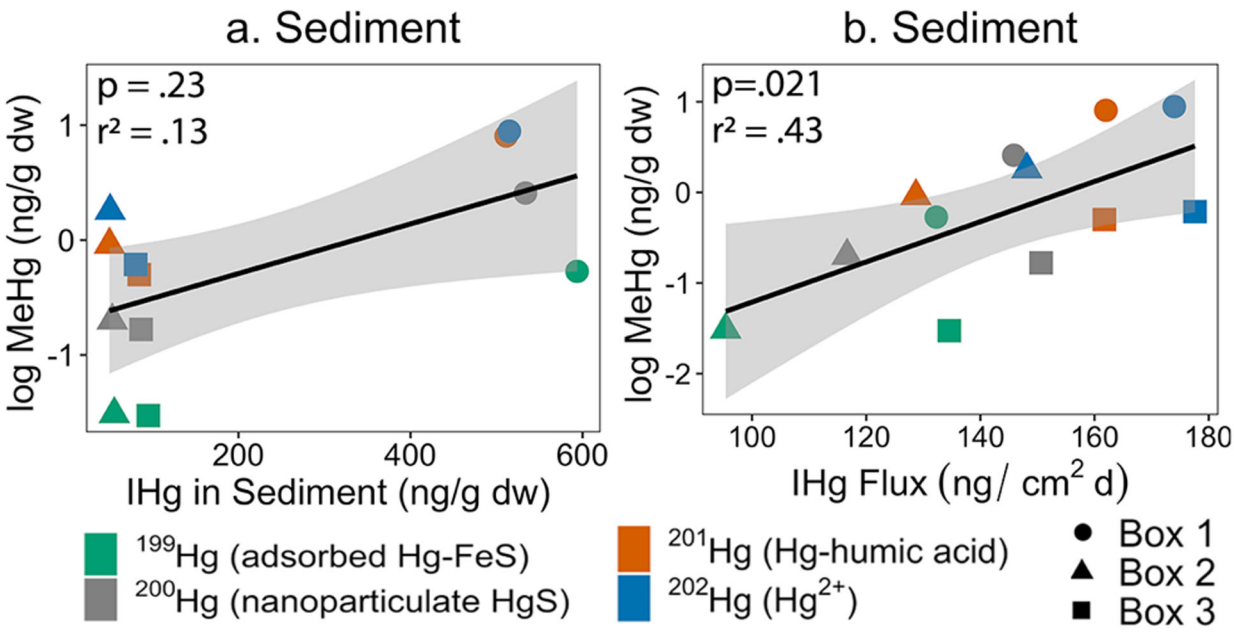

Figure 4.

Correlations between sediment MeHg content from each Hg isotope spike with respective IHg parameters: (left) sediment IHg content and (right) IHg flux into sediment-deployed DGT samplers. Each data point represents the average of n=3 sediments and n=6 DGT samplers for each box.

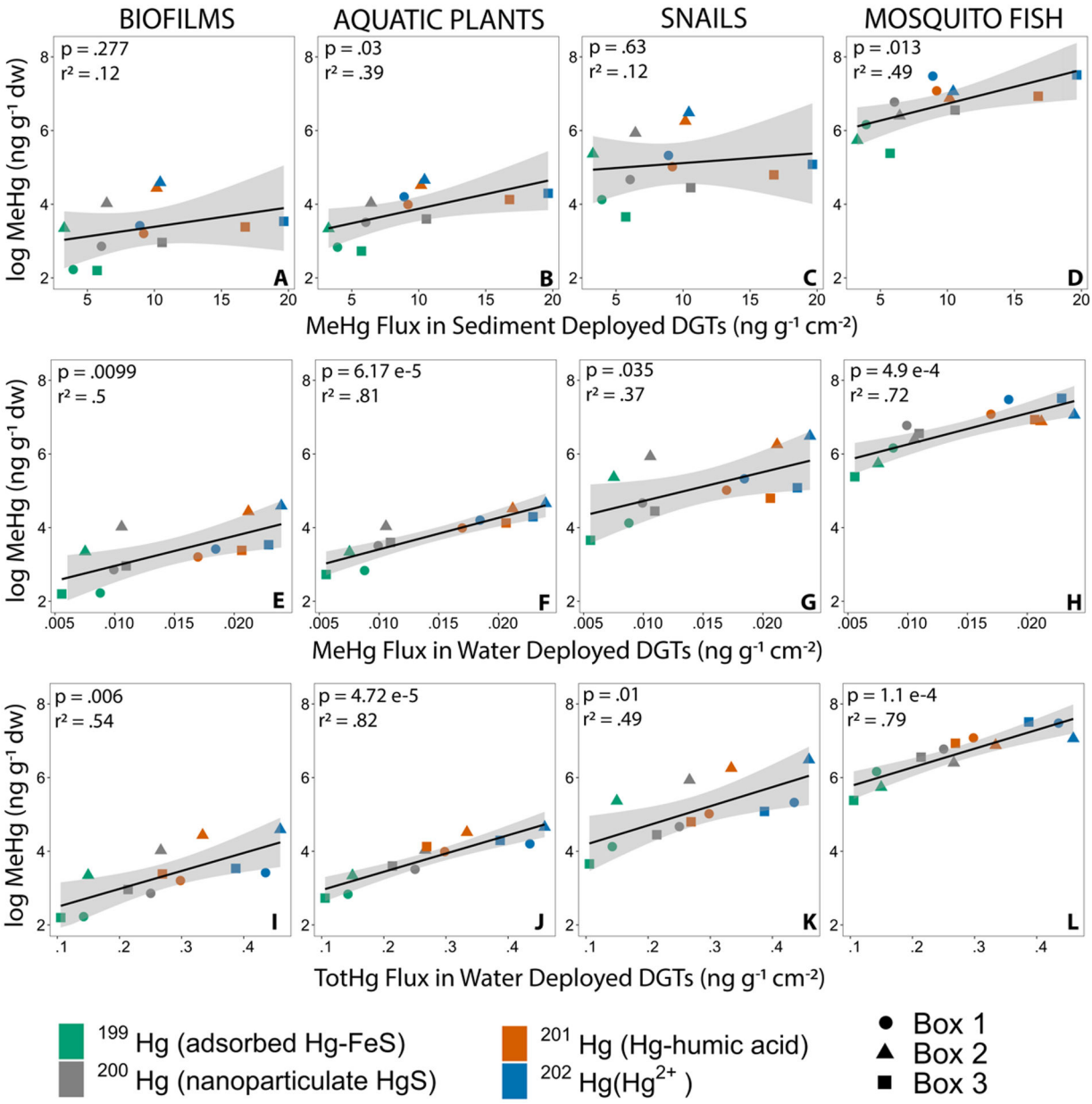

Figure 5.

Correlations between MeHg contents in Periphyton biofilms (column 1), *E. densa* plant stem and leaves (column 2), Snails (column 3), and Mosquitofish (*Gambusia* sp.) (column 4). Each row shows correlations with respective DGT parameters: (A-D) MeHg uptake flux in sediment deployed DGTs; (E-H) MeHg uptake flux in water deployed DGTs; (I-L) TotHg uptake flux into water deployed DGTs. Each data point represents the average of n=6 DGTs per box and n=4 macrofaunal specimen per box.